Journal of Agricultural Science and Engineering
Vol. 5, No. 1, 2019, pp. 14-23
http://www.aiscience.org/journal/jase
ISSN: 2381-6821 (Print); ISSN: 2381-6848 (Online)

Mathematical Modeling of Mass and Heat Transfer of Tomatoes in a Tunnel Dryer

Sana Ben Mariem[1, *], Slah Ben Mabrouk[2]

[1]National Research Institute for Rural Engineering, Water and Forestry (INRGREF), University of Carthage, Ariana, Tunisia
[2]Research and Technology Centre of Energy, Borj Cedria, (C.R.T.En.), University of Carthage, Hammam-Life, Tunisia

Abstract

In this study, numerical model for heat and mass transfer of granular products in a fixed-bed tunnel dryer was developed. A system of four differential equations constitutes the model structure. The obtained system of non-linear partial differential equations was numerically solved by a finite difference method. A computer code in FORTRAN language was written for the numerical solution of the problem. The drying process was simulated under real operating conditions based on a thin layer model and experimental drying kinetics. The numerical code allows establishing the profiles of temperature, absolute humidity, moisture content and drying front propagation of tomatoes slices spread out in a tunnel dryer of 10 m length, during the drying process. The obtained results were simulated for several operating conditions, the temperature and velocity of the drying air varied from 30°C to 70°C and 1m/s to 5m/s, respectively. The profile showed an evolution in temperature around an asymptotic limit which is the temperature of the drying air. Drying is manifested by the drying front propagation from the upstream flow to the downstream one. This drying front has clearly appeared after a blowing time for 4 hours. An abrupt increase of product temperature is followed. The drying time is shorter when the temperature is high, which is explained by the increase in the potential exchange between the air and the product. The model was validated by comparing experimental values of tomatoes in a thin layer with numerical simulations.

Keywords

Tunnel Dryer, Moisture Content, Mathematical Model, Numerical Simulation, Tomatoes

Received: January 28, 2019 / Accepted: March 10, 2019 / Published online: April 10, 2019

1. Introduction

Drying is one of the main techniques for preserving agri-food products. This is the most common process used to reduce the amount of water present in these products, so that the storage conditions are the most favorable.

Through this process, water activity decreases considerably during storage, as well as microbiological activity, with physical and chemical changes being minimized. Drying fruits or vegetables is a very delicate operation. The demand for agri-food products has become quite considerable in quantity and quality. The development of science and technology must meet the needs of contemporary man.

Furthermore, the drying of agri-food products is carried out in increasingly sophisticated dryers who allow a rational operation of the operation.

The drying air is constantly controlled in terms of speed, temperature and humidity so as to ensure rapid and efficient drying which does not alter the qualities of the product. These drying lines are often based on empirical results. They can be refined if we are better acquainted with the simultaneous evolution of heat and moisture transfers within the product and at the air-product interface. Thus, the study of the tunnel dryer consists in establishing on the one hand a

* Corresponding author
E-mail address: benmeriem.sana@gmail.com (S. B. Mariem)

relationship between the characteristics of the air at the inlet and at the outlet of the tunnel and on the other hand an equation between the drying time and The characteristics of the product layer.

The problems posed by the drying of the porous granular media relate to unsteady transfers of heat and mass.

The understanding of these transfer mechanisms will be very useful for the interpretation of phenomena specific to natural or forced convection. The description of heat and mass transfer in granular media is a consequence of the air-product interaction. The behavior of air and product will be translated into a mathematical model [1].

The aim of this work is to simulate the operating conditions of this dryer by a model based on a physical analysis carried out on two scales, the scale of the product and the scale of the tunnel as a whole. The model makes it possible, from the obtained drying curves, to determine, within the tunnel, the temperature, air humidity and product moisture content profiles for given operating conditions. It was thus possible to follow the drying sequences and compare our numerical results with those obtained experimentally.

2. Materials and Methods

The product used in this study is tomatoes to be dried in a solar dryer.

The solar dryer is located at the Laboratory of Energy and Thermal Processes, Center of Research and Technology of the Energy (CRTEn) in Borj Cedria. It is a tunnel dryer partially solar heating, (figure 1) designed to dry the agricultural products (tomatoes, carrots, apples, grapes, rosemary...)

The tomatoes are of the elongated type bought fresh from the local market and are homogeneous of approximately the same size

After washing with fresh water to remove impurities, residues of insecticides and other contaminations, the tomatoes were cut in half in the median plane and then spread on a metal tray of the drying chamber, the mass of the product to be dried Is 1200 g per tray.

The solar collectors aspirate fresh air which will be heated and routed to the pipes to be injected into the drying chamber.

In order to ensure a better stability of the drying conditions and a homogenization of the temperature inside the tunnel, the whole apparatus must be operated for at least half an hour before the tomatoes are introduced into the drying chamber. Drying was carried out at 50°C, 60°C and 70°C.

The wet mass of the product is taken every 20 min until a wet mass corresponding to a final water content of 11% is reached. The contents of each rack are weighed out of the dryer.

Figure 1. Photo of the drying device.

3. Mathematical Modelling

3.1. Identification of Physical Phenomena

The low temperature drying of products is very important in the field of agro-food industries.

The drying air is constantly controlled in speed, temperature and humidity in order to ensure fast and efficient dryingwhich does not affect the product qualities.

These drying lines are often based on empirical results.

They will be refined if we know better the simultaneous evolution of heat and moisture transfers within the product and at the air-product interface.

Thus, the study of the tunnel dryer consists in establishing on the one hand a relation between the characteristics of the air at the inlet and at the outlet of the tunnel and on the other hand an equation between the drying time and the characteristics of the product layer.

The problems posed by the drying of the porous granular media relate to unsteady transfers of heat and mass.

The understanding of these transfer mechanisms will be very useful for the interpretation of phenomena specific to natural or forced convection. The description of heat and mass transfer in granular media is a consequence of the air-product interaction. The behavior of air and product will be translated into a mathematical model [1].

3.2. Assumptions

To allow the development of a mathematical model describing the different physical phenomena during a drying process, simplifying assumptions are taken into account:

1) The convective heat exchange between the two phases is expressed using a volumetricheat transfer coefficient which depends on the airflow velocity and the texture of the porous medium.

2) The density of the air is constant.

3) The thermal conduction in the air and between the product sample is expressed using thermal conductivities equivalent coefficients of the solid and the fluid.

Given these assumptions, the temperature field T (x, t) and the moisture content X (x, t) can be determined by the system of partial differential equations [2].

3.3. Equations

The complex system can be represented as shown in figure 2.

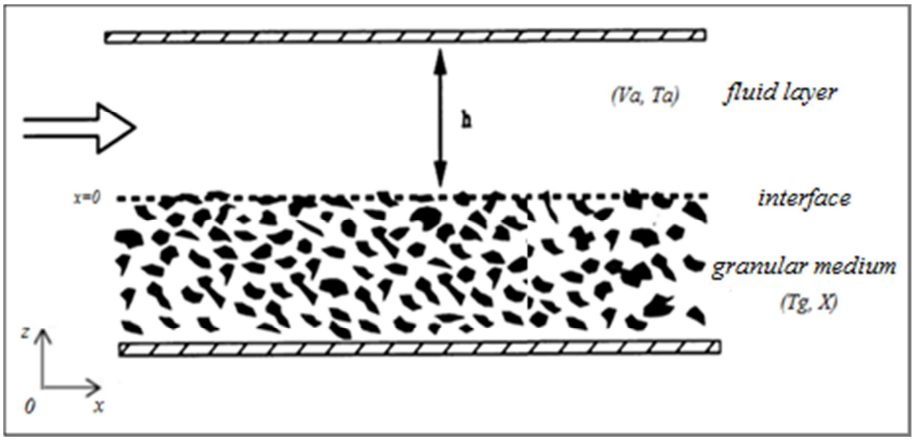

Figure 2. Schematic of a static tunnel dryer.

Interface Fluid-porous granular medium

The drying air, characterized by T_a and V_a, passes through the product layer which is at a moisture content X and at a temperature T_g (less than T_a) for a time interval Δt. So, a transfer of heat takes place from the air to the product due to the thermal deviation and a material transfer in the reverse direction under the effect of the water vapor pressure difference between the air and the surface of the product.

Consequently, a moisture content ΔX evaporates to the air whose relative humidity increases by ΔY and the temperature decreases by ΔTa (depending on the increase of the grain temperature ΔT_g) [2].

Air mass conservation equation

The increase in the absolute humidity of the air Y results from the water loss ΔX of the product:

$$\rho_a \left[\varepsilon \frac{\partial Y}{\partial t} + V_a \frac{\partial Y}{\partial x}\right] + (1-\varepsilon)\rho_g \frac{\partial X}{\partial t} = 0 \quad (1)$$

Air enthalpy conservation equation

The variation of the enthalpy of the airduring the crossing of the product layer is equal to the sum of the power exchanged by convection and evaporation at the product level:

$$\rho_a(C_a + YC_v)\left[\varepsilon \frac{\partial T_a}{\partial t} + V_a \frac{\partial T_a}{\partial x}\right] = \xi\alpha(T_g - T_a) - (1-\varepsilon)\rho_g C_v (T_g - T_a)\frac{\partial X}{\partial t} \quad (2)$$

Product enthalpy conservation equation

The variation of the enthalpy of the product is equal to the sum of the powers exchanged by convection with the air and of the energy used to vaporize the water of the product:

$$\rho_g(1-\varepsilon)(C_g + XC_w)\frac{\partial T_g}{\partial t} = \xi\alpha(T_a - T_g) + L_v\rho_g(1-\varepsilon)\frac{\partial X}{\partial t} \quad (3)$$

$$L_v = L^{\circ} + (C_v - C_w)T_g \quad (4)$$

Lv is the latent heat of vaporization at the temperature T_g.

L° is the latent heat of vaporization at the reference temperature 0°C.

On the upper side of a layer of the product, heat exchanges are not known. The existing flow above the porous surface is very complex. On the one hand, the face of the granular layer in contact with the hot air triggers two movements of heat and mass convection. On the other hand, the metal edges of the tunnel certainly influence the cellular structure of this flow [3].

Drying kinetics equation: Product mass conservation equation

To these equations we must add the Drying kinetics equation which represents the mass balance for the product.

$$\left(-\frac{dX}{dt}\right) = X_{in}F(X_r) \quad (5)$$

$$F(X_r) = A_0 + A_1X_{r+}A_2X_r^2 + A_3X_r^3 \quad (6)$$

The development of this system of equations leads to the analytic solution of the static dryer.

In that case, simplifying assumptions can be considered [4] and [5]:

i. The conduction heat transfer is negligible compared to that by convection.

ii. The flow is unidirectional.

iii. The air inlet conditions are constant.

iv. The air flow is constant and uniform along the tunnel.

v. The unsteady terms in the air mass conservation and the air enthalpy conservation equations are negligible, except for drying, i.e.:

$$\varepsilon \frac{\partial Y}{\partial t} \ll V_a \frac{\partial Y}{\partial x} \text{et} \varepsilon \frac{\partial T_a}{\partial t} \ll V_a \frac{\partial T_a}{\partial x} \quad (7)$$

vi. The term sensible heat is negligible compared to that of the latent heat:

$$(C_v - C_w)T_g \ll L^{\circ} \text{et} Y C_v \ll C_a \quad (8)$$

vii. The sensible heat flux of evaporated water is neglected compared to the convicted heat flux air-product:

$$(1-\varepsilon)\rho_g C_v \frac{\partial X}{\partial t} \ll \xi\alpha \quad (9)$$

The system of preceding equations then becomes:

Air mass conservation equation:

$$\rho_a V_a \frac{\partial Y}{\partial x} = -(1-\varepsilon)\rho_g \frac{\partial X}{\partial t} \quad (10)$$

Air enthalpy conservation equation:

$$\rho_a C_a V_a \frac{\partial T_a}{\partial x} = \xi\alpha(T_g - T_a) \quad (11)$$

Product enthalpy conservation equation:

$$-\xi\alpha(T_a - T_g) = L^0 \rho_g (1-\varepsilon) \frac{\partial X}{\partial t} \quad (12)$$

Total enthalpy conservation equation for air and product:

$$\rho_a C_a V_a \frac{\partial T_a}{\partial x} = L^0 \rho_g (1-\varepsilon) \frac{\partial X}{\partial t} \quad (13)$$

3.4. Model Transfer Coefficients

The model developed requires knowledge of different parameters. Some are identified (physical characteristics of air and water) and others are less known (transport parameters related to the product). This leads to the use of empirical relationships in the literature.

The main numerical data necessary for the simulation are presented in the table 1.

Table 1. Parameters and constants used for the simulated processes.

Product characteristics	X: moisture content (kg kg^{-1} dry basis) = *12 kg/kg* Cp: product specific heat capacity = *4180 J/kg°C* σ: product area density = *3 à 5 kg/m^2*
Drying air characteristics	Ca: air specific heat capacity = *1006 J/kg°C* Cv: vapor specific heat capacity = *1840 J/kg°C* Air temperature (K or°C): *30°C <Ta < 70°C* Va: air velocity = *1 m/s à 5 m/s* Hr: ambient relative humidity = *5% à 40%* ξ: solid–gas transfer area = 36 à 40 m^2/m^3 l: tunnel lenght = *10 m*
Dryer characteristics	h: fixed bed height = 0.01 m A: bed area = *1 m^2* X_{nc}: Commercial standard of final moisture content = *0.16 kg/ kg (dry basis)*

3.5. Initial and Boundary Conditions

This system, although translating laws governing the heat and moisture flow in the product, can be solved only if it know both:

1. -the initial state of the product is the initial temperature and the initial moisture content. These data are called initial conditions.
2. the boundary conditions are the expression of the exchanges between the product and the air; exchanges that are on the surface of the product, also called product–airdrying interface.

Initial conditions

Initially, the porous medium is assumed to be isothermal and in hydrostatic equilibrium. The state of the system is then described by:

$$\begin{cases} X(x;0) = X_{in} \; et \; T_a(x;\,0) = T_a \\ Y(x;0) = Y_{in} \; et \; T_g(x;\,0) = T_{am} \end{cases}$$

Boundary conditions

The configuration of the tunnel entrance section leads to the following limit conditions:

$$\begin{cases} X(0;t) = X_0 \; et \; T_a(0;\,t) = T_{a0} \\ Y(0;t) = Y_0 \; et \; T_g(0;\,t) = T_{g0} \end{cases}$$

3.6. Resolution Method

The system of equations is described by partial differential equations highly coupled and nonlinear. In general, these equations do not admit analytical solutions except in very simplified cases. This is why it is necessary to use numerical methods of resolution.

There are several numerical methods: a finite difference method -finite volume method -finite element method -spectral method... Each method of numerical resolution includes a meshing phase and a discretization phase.

The meshing phase consists of dividing the field of study into small volumes called control volumes. The discretization phase transforms the continuous problem into a discrete problem. Equations and boundary conditions are approximated by equations and discrete conditions.

In this work, the above system of equations is solved by the finite difference method using a volume control approach [6].

The advantage of this method is the great simplicity of writing and the low computational cost.

To solve a differential equation of the system, we build a mesh consisting of a grid of equidistant meshes (nodes) Δxi. Around each point, we defines a control domain, then we integrates the equation on this domain according to a time step Δt and a space step Δxi.

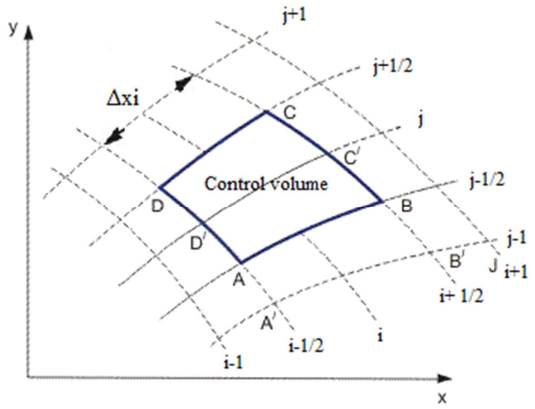

Figure 3. Numerical network grid.

The discretization of the equations is made assuming the following considerations:

The value of a physical quantity Φ (generic of Ta, X, Yg or Ya) at any point i and at time n is noted as Φ_i^n

The first derivatives in space are approximated by a developing Taylor series to the order 2, around points (i-1/2) and (i + 1/2).

We have:

$$\frac{\Phi_{i+1/2}^n - \Phi_{i-1/2}^n}{\Delta x} = \left(\frac{\partial \Phi}{\partial x}\right)_i^n + \phi(\Delta x^2) \qquad (14)$$

The nonlinear and coupled character of the equations is treated by an iterative technique of finite difference based on a calculation procedure of $(\Phi)_{i+1/2}^{n+1}$ known and $(\Phi)_{i+1}^{n+1}$ estimated. The value of Φ at the instant (n + 1/2) is determined by the interpolation of the values relating to the instants (n) and (n + 1), from where:

$$\frac{\Phi_{i+1/2}^n - \Phi_{i+1/2}^{n+1}}{2} = (\Phi)_{i+1/2}^{n+1/2} \qquad (15)$$

Transport parameters (α, λ, βm...) are evaluated by assuming their linear variations between two neighboring nodes on the faces of the control domain. On the faces of the physical domain (extreme points i = 1 and i = M), the discretization of the equations is obtained by integrating on one half of the control volume and taking into account the boundary conditions.

The convergence test imposes the following condition for each variable:

MAX $|\Phi_{k+1}| < \delta$ where δ is "infinitely small" and $\Delta\Phi_{k+1}$ being the evolution of Φ between two successive iterations.

The calculations are organized by a program developed in FORTRAN language. In a first calculation step, the time and space steps are kept constant as long as no convergence problem arises.

For each time step, the iterations start from an estimated state and stop when the convergence criteria are satisfied. If for a given time step, the calculations do not converge after a threshold of iterations, the two temporal and spatial meshes are then refined. This situation is only encountered when the complete system is solved.

To solve the simplified system, we chose a regular spatial mesh.

On the other hand, the temporal mesh is variable, the time step Δt chosen initially very small, and increases progressively in order to follow the development of product characteristics.

Moreover, when the superficial evaporation disappears, a drying front appears at the product layer. To better follow its displacement, it is important to use a variable mesh in space and time.

4. Results

4.1. Validation of the Numerical Model

The model presented has been validated in the Thermal Processes Laboratory at the CRTEn by previous numerical and experimental work on different agricultural products [7].

However, to assess the model's capacity to describe the different drying profiles, it seemed useful to compare the numerical solutions with the experimental results obtained with the solar dryer.

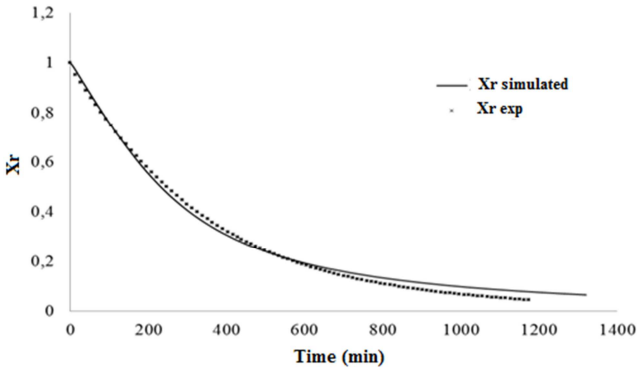

Figure 4. Evolution of experimental and simulated moisture contents of tomato samples with a thickness of 1 cm (T = 50°C, V = 2 m / s).

Figure 4 shows the evolution of experimental and simulated reduced moisture contents as a function of time.

The numerical and experimental results present a close agreement, validating the model presented.

4.2. Results of the Numerical Simulation

The numerical evaluation of this model makes it possible to establish the profiles of the temperatures, the absolute humidity and the moisture content during the drying. It also makes it possible to follow the displacement of the drying front for different starting conditions.

In order to analyze the influence of inlet air properties on drying, we studied the evolution of the temperature T (x, t) of the air and of the product and of the moisture content X (x, t) of the tomatoes slices spread in a tunnel dryer of length 10 m, subjected to different climatic conditions.

The simulation results obtained for different operating conditions are presented below with the OriginPro8 software.

The different curves represent at different moments a photograph of the spatial evolution of temperatures, absolute humidity and moisture content during drying. All curves are subject to strong disturbances.

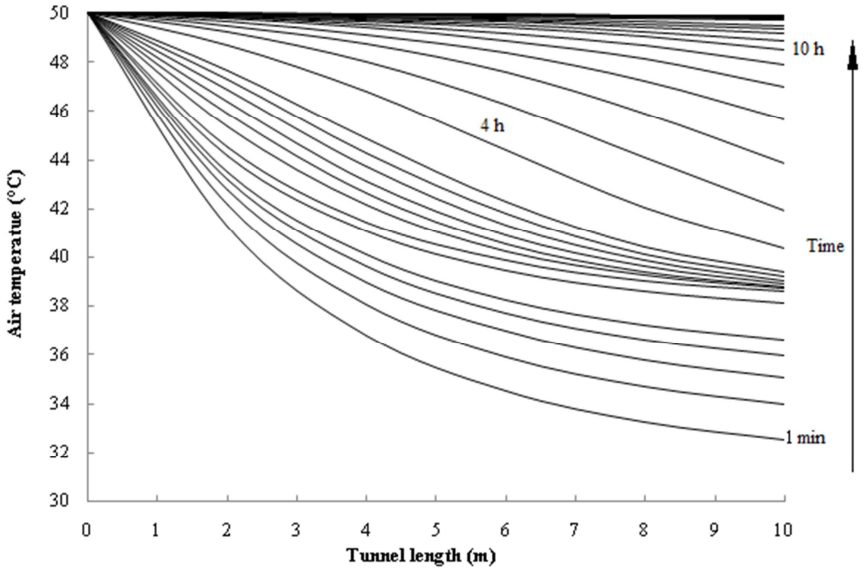

Figure 5. Air temperature evolution as a function of the tunnel length during drying at 50°C.

Drying conditions: T_a=50°C, T_{am}=28°C, V_a=2m/s, RH =5%, X_{in}=12kg/kg. db, X_{eq}=0.05kg/kg. db

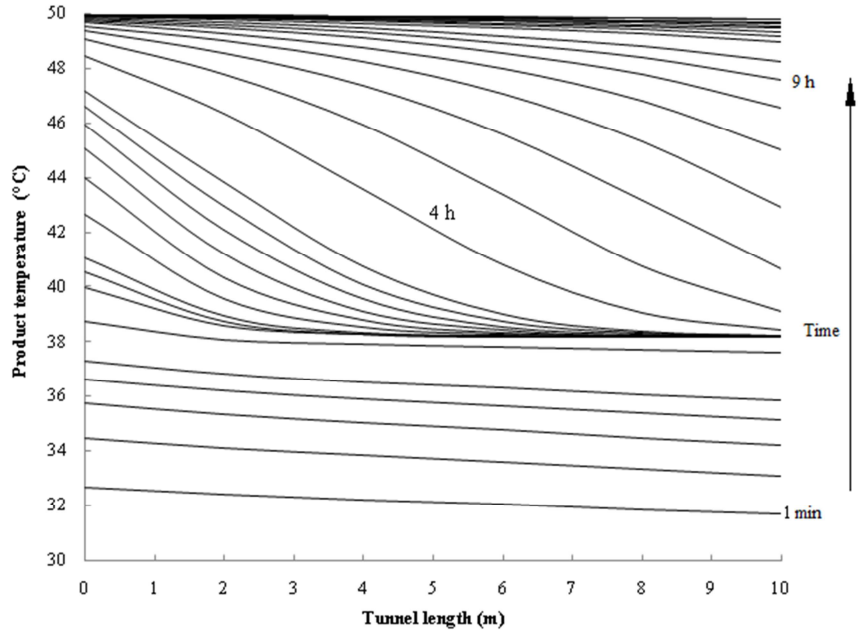

Figure 6. Product temperature evolution as a function of the tunnel length during drying at 50°C.

Drying conditions: T_a=50°C, T_{am}=28°C, V_a=2m/s, HR=5%, X_{in}=12kg/kg.db, X_{eq}=0.05kg/kg.db

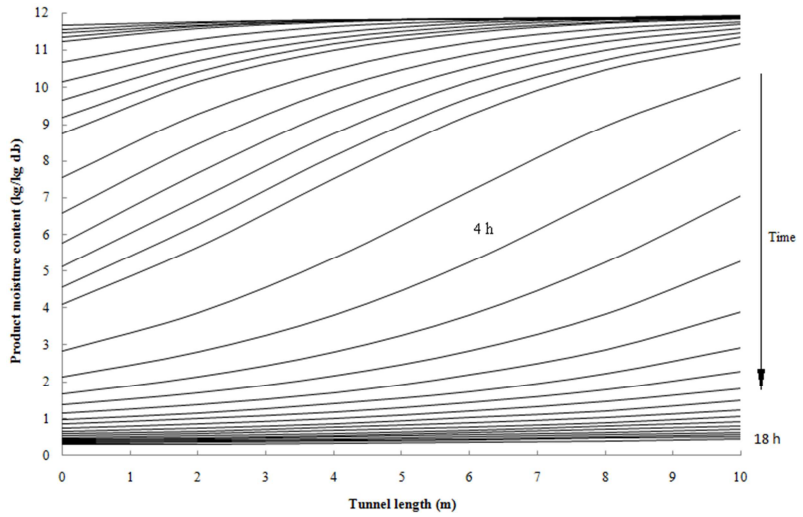

Figure 7. Product moisture content evolution as a function of the tunnel length during drying at 50°C.

Drying conditions: T_a=50°C, T_{am}=28°C, V_a=2m/s, RH=5%, X_{in}=12kg/kg.db, X_{eq}=0.05kg/kg.db

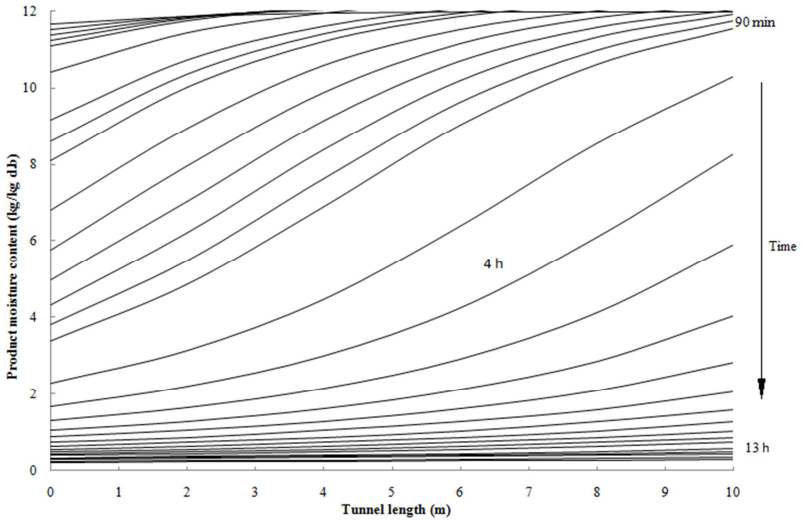

Figure 8. Product moisture content evolution as a function of the tunnel length during drying at 70°C.

Drying conditions: T_a=70°C, T_{am}=27°C, V_a=2m/s, RH=5%, X_{in}=12kg/kg.db, X_{eq}=0.05 kg/kg.db

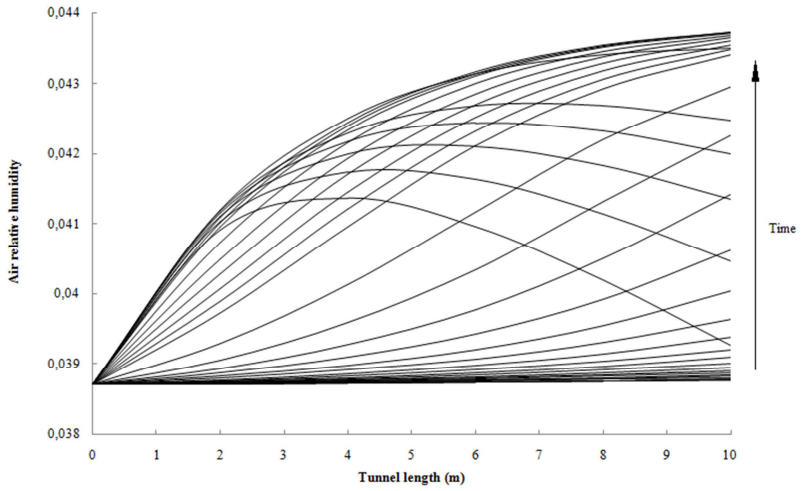

Figure 9. Air relative humidity evolution during drying as a function of the tunnel length at 50°C.

Drying conditions: T_a=50°C, T_{am}=28°C, V_a=2 m/s, RH=5%, X_{in}=12kg/kg.db, X_{eq}=0.05 kg/kg.db

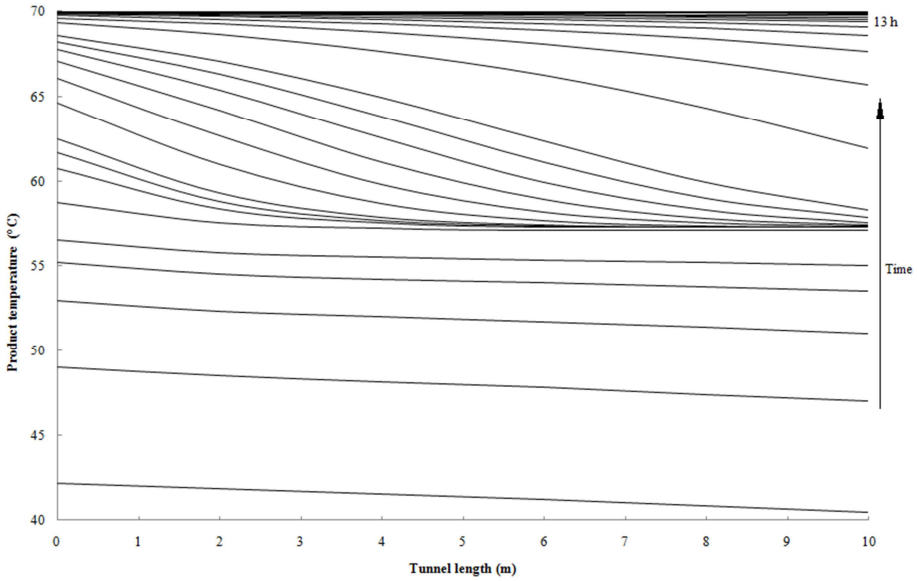

Figure 10. Product temperature evolution as a function of the tunnel length during drying at 70°C.

Drying conditions: T_a=70°C, T_{am}=28°C, V_a=5m/s, RH=5%, X_{in}=12 kg/kg.db, X_{eq}= 0.05kg/kg.db

The profile shows a temperature evolution towards an asymptotic limit which is the temperature of the drying air.

The drying is manifested by the displacement of the drying front from the upstream to the downstream of the flow (figures 5 to 10).

This drying front appears clearly after a certain blowing time of 4 hours. It is followed by an abrupt increase in the product temperature, which shows that the drying temperature is an important parameter to consider.

The drying time is shorter when the temperature is high, which is explained by the increase in the exchange potential between the air and the product, thus promoting the evaporation of the product water.

The beginning of the second drying phase is characterized by a slight distortion of the moisture content profiles. It has been found that the speed of movement of the drying front initially variable tends progressively to a constant value.

After a short transitional phase during which the medium cools down to the wet temperature Th, a short phase at a constant drying speed begins.

During this phase, transport is only a transport of liquid water to the surface.

The vapor flow inside the product layer is almost equal to zero. The equilibrium between the thermal energy supplied by the drying air and the energy used for evaporation allowed to express the drying velocity in the first phase.

Figure 11 shows the space-time evolution of the relative difference temperature, $DT^* = (T_a - T_g) / (DT_{ref})$, between the product temperature and the air temperature calculated in a tunnel of 10 m length.

For this study, D_{ref} is an interval between the reference temperatures which is equal to 27°C for the air temperature 50°C.

In the beginning, the relative difference of temperature DT* is important only at the inlet of the tunnel because the inlet temperature is higher than the initial product temperature.

After that, there is a difference only in the region where the evaporation front is located. This is due to the difference between the product thermal characteristics and the hot air.

As time goes on, the overheating propagates inside the medium. The product temperature and the moisture content tend to their final values in the whole of the medium, and evaporation ceases (Figures 6 and 7).

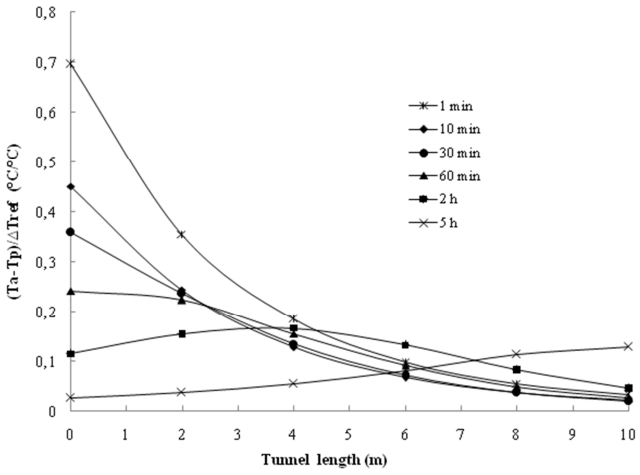

Figure 11. Space-time evolution of the relative difference of temperature between the product and the air temperature at 50°C.

From average moisture content, the capillary forces which supply the surface with liquid water become insufficient and an evaporation front appears; this is the beginning of a phase with decreasing drying speed. The vapor flow becomes important near the evaporation front, moving progressively to the downstream of the tunnel (figure 7). The absorbed heat flux is no longer compensated by the mass flow and the drying process is controlled by the internal parameters of the porous medium [8].

It should be noted that with the same product dried in a thin layer, it can be observed in some cases, differences on the shape of the drying kinetics. These differences may arise from several effects:

The "screen" effect due to the contamination of the surface by hygrophobic substances.

This pollution of the surface results in a change in surface tension and especially a reduction in the wet surface area.

The "2D" effect which occurs when the boundary layer is not uniform over the width of the tunnel. In a two-dimensional calculation in a porous medium, Plumb and Prat showed that the 2D effect could be the cause of the appearance of a premature period with decreasing drying speed [9].

These observations led to the following hypotheses:

Hypothesis 1: The mathematical model used is correct, but the choice of a regular spatial mesh is inadequate. Indeed, as noted above, if the appearance of a drying front is possibly situated between two adjacent points of the mesh, we can imagine that this regular mesh would have masked certain phenomena of the front.

Hypothesis 2: Some physical phenomena are perhaps not considered in the writing of the model, especially the simplified model. Indeed, during the implementation of this model, we have noticed that the beginning of a drying operation is characterized by a varied movement of the drying front.

For the first hypothesis, we have taken the calculations with finer meshes.

However, we have not noticed any notable improvements in the drying kinetics. This hypothesis was therefore rejected.

The second hypothesis deserves a more detailed examination such as the need to introduce variable coefficients of exchange to account for the reduction of the wet surface, or the redefinition of certain parameters of the model. Some possible interpretations can be envisaged:

To assume the existence of a phenomenon of evaporation-condensation which has taken place on a microscopic scale and which causes the moisture in vapor form to be directed against the drying front. This makes it possible to assert that the mobility of water is very low in this zone and the problem deserves a priori to be posed.

Challenging the validity of the model and its constituent hypotheses to favor a more sophisticated and complicated model of knowledge. Such a choice would then be a challenge.

5. Conclusion

The theoretical and numerical study carried out in this study made it possible to appreciate the capacity of the model to describe the different phases of drying of a biological material. Due to the results obtained, it can be said that this model makes it possible to successfully simulate the appearance and then the evolution of the drying phases. The agreement between the results of the numerical simulation and those obtained experimentally remains sometimes unsatisfactory.

There is sometimes a discrepancy between simulation results and experimental results. To explain this difference, it is necessary to make the following remarks:

1. The convective heat exchange coefficients between the product and the drying air are not all well known, in fact the coefficient of convective exchange is taken constant for a given air velocity whereas it should vary according to changes in product temperature.
2. The simplifying hypotheses considered also contribute to the explanation of the observed difference between the temperature profiles (phenomenon of radiation and conduction neglected).
3. The initial conditions taken in the model do not always provide a good approximation of reality.
4. Experimental problems may be present, for example, linked to thermocouples.

References

[1] Masmoudi W., 1990. Contribution à l'étude fondamentale du séchage des matériaux cappillario-poreux: Cinétique de la modélisation macroscopique et du protocole expérimental de validation. Thèse de Doctorat, Institut National Polytechnique de Toulouse.

[2] Ben Mabrouk S., 1999. Etude des transferts simultanés de chaleur et de masse dans les milieux poreux: Modélisation des phénomènes de séchage, Thèse de doctorat, Faculté des sciences de Tunis, 240 p.

[3] Ben Mabrouk S., Arnaud G., Fohr J-P., Belghith A., 1989. Etude du séchage en couche mince de produits agricoles. J. I. Th, (.2, 471 - 480.) Actes des Journées Int Thermique J. I. T. H '89'. 2 (1), 471 - 480, Edition CNRS, Paris.

[4] Boukadida N., Perre P., Ben NasrallahS., 2000. Mechanism of two dimensional heat and mass transfer during convective drying of porous media under different drying conditions, Drying Technol. 18 (7) pp 1367–1388.

[5] Arnaud G., Fohr J. P., 1988. Slow drying simulation in thick layers of granular products, Int. J. Heat Mass Transfer 31 (12) pp 2517– 2526.

[6] Patankar S. V., 1981. Numerical Heat Transfer and Fluid Flow, Hemisphere Publication corporation New York, 193 p.

[7] Ben Mabrouk S., Belghith A., 1994. Simulation and design of a tunnel drier, Renew. Energy 5 (1) pp 469–473.

[8] Ben Mabrouk S., Azzouz S., Guizani A., Belghith A., 1991. Modélisation des transferts de chaleur et de masse lors du séchage de produits granulaires. Proc. 5th International Meeting on Heat Transfer. 2, pp 417-480.

[9] Plumb O., Prat M. (1992), Microscopic model for the study of drying of capillary porous media. Drying 92, 397-406.